

## Apigenin sensitizes doxorubicin-resistant hepatocellular carcinoma BEL-7402/ADM cells to doxorubicin via inhibiting PI3K/Akt/Nrf2 pathway

Ai-Mei Gao<sup>1,2</sup>, Zun-Ping Ke<sup>3</sup>, Jia-Ning Wang<sup>4</sup>,  
Jian-ye Yang<sup>4</sup>, Shi-You Chen<sup>5</sup> and Hui Chen<sup>1,\*</sup>

<sup>1</sup>Department of Pharmacology, Tongji Medical College, Huazhong University of Science and Technology, Wuhan, Hubei 430030, China, <sup>2</sup>Laboratory of Chinese Herbal Pharmacology, Renmin Hospital, Hubei University of Medicine, Shiyan, Hubei 442000, China, <sup>3</sup>Department of Cardiology, The Fifth People's Hospital of Shanghai, Fudan University, Shanghai, China, <sup>4</sup>Institute of Clinical Medicine and Department of Cardiology, Renmin Hospital, Hubei University of Medicine, Shiyan, Hubei 442000, China and <sup>5</sup>Department of Physiology and Pharmacology, University of Georgia, Athens, GA 30602, USA

\*To whom correspondence should be addressed. Tel/Fax: +86 27 83692628; Email: [chenhuijmu@163.com](mailto:chenhuijmu@163.com)

**Nuclear factor erythroid 2-related factor 2 (Nrf2) is a redox-sensitive transcription factor regulating expression of a number of cytoprotective genes. Recently, Nrf2 has emerged as an important contributor to chemoresistance in cancer therapy. In the present study, we found that non-toxic dose of apigenin (APG) significantly sensitizes doxorubicin-resistant BEL-7402 (BEL-7402/ADM) cells to doxorubicin (ADM) and increases intracellular concentration of ADM. Mechanistically, APG dramatically reduced Nrf2 expression at both the messenger RNA and protein levels through downregulation of PI3K/Akt pathway, leading to a reduction of Nrf2-downstream genes. In BEL-7402 xenografts, APG and ADM cotreatment inhibited tumor growth, reduced cell proliferation and induced apoptosis more substantially when compared with ADM treatment alone. These results clearly demonstrate that APG can be used as an effective adjuvant sensitizer to prevent chemoresistance by downregulating Nrf2 signaling pathway.**

### Introduction

Hepatocellular carcinoma (HCC) is the fifth most prevalent malignant diseases and the third leading cause of cancer-related deaths in the world (1). Despite the fact that several new chemotherapeutic drugs have been developed and a number of aggressive treatments are available, cancer death rate continues to rise. A major factor causing the failure of cancer therapy is the resistance to therapies including chemoresistance.

Nuclear factor erythroid 2-related factor 2 (Nrf2) is originally identified as a pivotal factor for cell protection from oxidative and electrophilic insults. Nrf2 regulates the expression of various cytoprotective genes by binding to antioxidant-response elements (AREs) in the promoters of the corresponding genes such as heme oxygenase-1 (HO-1), NAD(P)H: quinone oxidoreductase 1, aldo-keto reductases and several adenosine triphosphate-dependent drug efflux pumps (2,3).

Kelch-like ECH-associated protein 1 (Keap1), a substrate adaptor protein for a Cul3-dependent E3 ubiquitin ligase complex, is a major repressor of Nrf2 (4). Keap1 constitutively suppresses Nrf2 activity in the absence of stress. However, oxidants and electrophiles hamper the Keap1-mediated proteasomal degradation, resulting in stabilization of

**Abbreviations:** ADM, doxorubicin; APG, apigenin; DAPI, 4',6-diamidino-2-phenylindole; FCM, flow cytometry; HCC, hepatocellular carcinoma; HO-1, heme oxygenase-1; Keap1, Kelch-like ECH-associated protein 1; mRNA, messenger RNA; MRP5, multidrug resistance-associated protein 5; MTT, 3-(4,5-dimethylthiazole-2-yl)-2,5-diphenyl tetrazolium bromide; Nrf2, nuclear factor erythroid 2-related factor 2; PBS, phosphate-buffered saline; PI3K, phosphatidylinositol-3 kinase; Rh123, rhodamine 123; siRNA, small interfering RNA.

Nrf2 and subsequent transactivation of downstream genes regulating cell survival (5).

Recently, Nrf2 emerged as a potential pharmacological target for overcoming chemoresistance due to findings that Nrf2 overexpression enhances chemoresistance, whereas blockade of Nrf2 sensitizes a variety of cancer cells including neuroblastoma, breast, ovarian, prostate, lung and pancreatic cancer cells to chemotherapeutic drugs (6–10). Therefore, identification of small-molecule inhibitors that potently inhibit the Nrf2-dependent response is desirable, and such compounds may be used as an adjuvant sensitizer to combat chemoresistance.

AKR1B10, a human member of the aldo-keto reductase superfamily, is overexpressed in primary liver and lung carcinomas (11,12). AKR1B10 promotes cancer cell growth and survival through increasing lipogenesis and eliminating cytotoxic carbonyls and is thus considered as a tumor-promoting factor (13,14). Recent studies have demonstrated that AKR1B10 may be a key factor responsible for drug resistance in cancer cells (15,16). However, the study on its relationship with the HCC chemotherapy is very limited. Furthermore, although the induction of AKR1B10 by Nrf2 has been reported (13), it is unclear if the induction is involved in HCC resistance to chemotherapy.

Multidrug resistance-associated protein 5 (MRP5), a member of the ABC superfamily of transmembrane proteins, has been identified as a protective pump against endogenous and exogenous toxic agents. MRP5 is highly expressed in several drug-resistant cell lines to confer resistance to anticancer drugs, such as 5-fluorouracil, gemcitabine, cisplatin and methotrexate (17). However, molecular mechanisms that regulate MRP5 overexpression in cancer cells have not been defined. Because Nrf2 is a stress-inducible transcription factor, which regulates the expression of several cytoprotective genes and drug detoxification enzymes via a common ARE located in the promoter, we decided to investigate whether Nrf2 regulates the expression of MRP5 as well.

Flavonoids are polyphenolic compounds that occur ubiquitously in food plants and vegetables. Flavonoids are generally safe and are associated with low toxicity, making them ideal candidates for cancer chemopreventive agents. Several flavonoid compounds have been reported to be potent Nrf2 inhibitors, such as epigallocatechin 3-gallate, luteolin and brusatol (18–20). These prompted us to determine whether other flavonoids structurally related to them can sensitize cancer cells to anticancer drugs through inhibiting Nrf2 signaling pathway.

Apigenin (4',5,7-trihydroxyflavone, APG) is a natural bioflavonoid widely present in many fruits and vegetables. APG has various biological activities such as anti-inflammatory, antioxidant and anticarcinogenic properties (21). In this study, we report the identification of APG as a potent inhibitor of the Nrf2 pathway that sensitizes doxorubicin-resistant BEL-7402 cells (BEL-7402/ADM) to ADM, increases intracellular ADM level and suppresses tumor growth in a mouse xenograft model. Mechanistically, APG significantly reduced Nrf2 and its downstream genes expression through downregulating phosphatidylinositol-3 kinase (PI3K)/Akt pathway, resulting in a reversal of drug-resistant phenotype. Thus, APG is a promising dietary agent for inhibiting Nrf2 pathway to sensitize cancer to therapeutic drugs.

### Materials and methods

#### Reagents

APG was purchased from Shaanxi Huike Botanical Development (China) and ADM was purchased from Zhejiang Haizheng Pharmaceutical Co., Ltd (China). PI3K inhibitor (LY294002) was obtained from Beyotime Institute of Biotechnology (China). Nrf2, MRP5, Akt, phospho-Akt-Ser473 (p-Akt), ERK1/2, phospho-ERK1/2 (p-ERK1/2), P38, phospho-P38 (p-P38), JNK, phospho-JNK (p-JNK),  $\beta$ -actin and Lamin B antibodies were obtained from Santa Cruz Biotechnology (Santa Cruz, CA). AKR1B10

and HO-1 antibodies were from Epitomics (Burlingame, CA), horseradish peroxidase-conjugated goat anti-rabbit immunoglobulin G and fluorescein isothiocyanate-conjugated anti-rabbit immunoglobulin G antibodies were from Jackson ImmunoResearch Laboratories (West Grove, PA). HiPerFect Transfection reagent was from Qiagen (Valencia, CA). SYBR RT-PCR kits were from Toyobo (Japan), and 4',6-diamidino-2-phenylindole (DAPI), propidium iodide and rhodamine 123 (Rh123) were from Sigma (St Louis, MO). PV-9000 Kit was obtained from Zhongshan Goldenbridge Biotechnology (China). Trypsin, RPMI-1640 and TRIzol reagent were purchased from Gibco Invitrogen (Carlsbad, CA), and fetal bovine serum was purchased from Hangzhou Sijiqing Company (China).

*Cell culture*

The parental human HCC cells (BEL-7402) and BEL-7402/ADM cells were kindly provided by Prof. X.B.Wang of Hubei University of Medicine (China, Shiyan). BEL-7402 cells were cultured in RPMI-1640 medium containing 8% fetal bovine serum in a humidified incubator containing 5% CO<sub>2</sub> at 37°C. BEL-7402/ADM cells were grown in the above-mentioned medium with the addition of 2 μM ADM for at least 4 weeks prior to the experiment (22).

*MTT assay*

Cells were plated at a density of 4×10<sup>3</sup> cells/well in 96-well plates. After overnight recovery, BEL-7402/ADM cells were exposed to 10 μM of APG

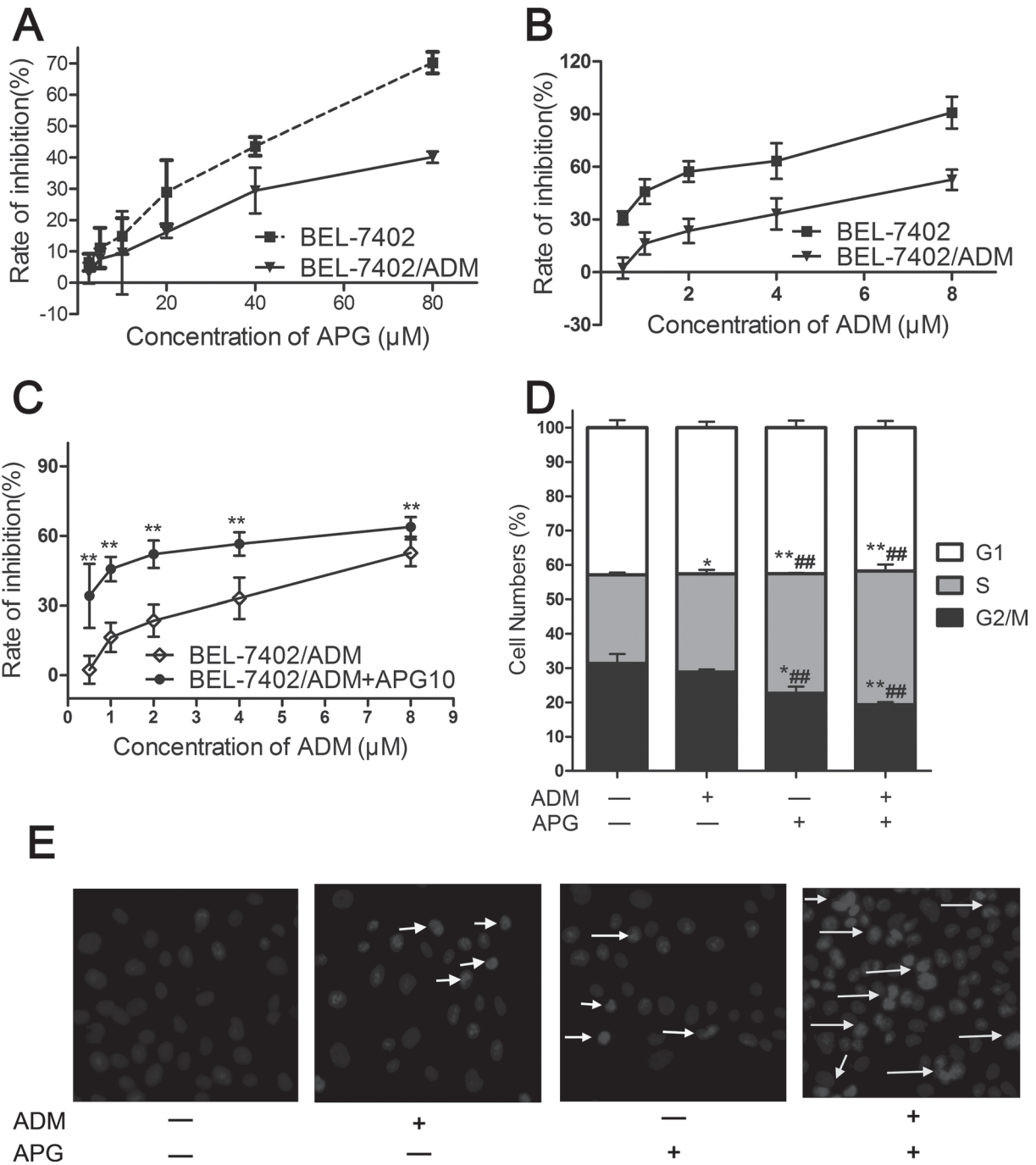


**Fig. 1.** APG increased the sensitivity of BEL-7402/ADM cells to ADM. (A–C) MTT assays. Cells were incubated for 48 h with increasing concentrations of APG (2.5–80 μM) (A), ADM (0.5–8 μM) (B) or with 10 μM of APG followed by 48 h exposure to ADM (0.5–8 μM) (C). \**P* < 0.05, \*\**P* < 0.01 compared with ADM alone-treated group. (D) Cells were treated with 20 μM of APG or/and 2 μM of ADM for 24 h. The treated cells were subjected to cell cycle analysis. \**P* < 0.05, \*\**P* < 0.01 versus untreated control cells; ##*P* < 0.01 versus cells with ADM treatment alone. (E) Cells were treated with 20 μM of APG or/and 2 μM of ADM for 24 h. Fluorescent staining of nuclei by DAPI. Condensed and fragmented nuclei and apoptotic bodies were indicated with arrows. All images are shown at ×200.

followed by 48h incubation in fresh culture medium containing ADM (0.5–8  $\mu\text{M}$ ). Then, 20  $\mu\text{l}$  of 3-(4,5-dimethylthiazole-2-yl)-2,5-diphenyl tetrazolium bromide (MTT) solution (2mg/ml) was added and incubated for 4h. After removal of the MTT solution, 200  $\mu\text{l}$  of dimethyl sulfoxide was added, and the absorbance at 570nm was measured.

#### Cell cycle analysis

Cells were fixed in 70% ice-cold ethanol at 4°C overnight. For cell cycle analysis, the cells were treated with 100  $\mu\text{g/ml}$  of RNase A at 37°C for 30min, stained with 50  $\mu\text{g/ml}$  of propidium iodide at 4°C for 30 min and then analyzed for DNA content by flow cytometry (FCM).

#### DAPI staining assay

Cells were fixed in 4% paraformaldehyde for 20 min and permeabilized by sequentially treating with 0.3% Triton X-100 for 20 min. A 200  $\mu\text{l}$  of DAPI solution (1  $\mu\text{g/ml}$ ) was added into each well and incubated at room temperature for 10 min in dark. The sections were visualized using a fluorescence microscope.

#### Intracellular accumulation of ADM assay

Cells were pretreated with 10 or 20  $\mu\text{M}$  of APG for 24 h and then incubated with 8  $\mu\text{M}$  of ADM at 37°C for 3 h. After washing with phosphate-buffered saline (PBS), the cells were subjected to fluorescence microscopy and FCM with the excitation wavelength at 488nm and emission wavelength at 575 nm.

#### Rh123 accumulation assay

Cells were preincubated with APG for 24h and then exposed to 5  $\mu\text{g/ml}$  of Rh123 at 37°C for 1 h. After washed with ice-cold PBS, the cells were immediately subjected to FCM to measure the green fluorescence signal produced by Rh123.

#### Nrf2 small interfering RNA transfection

A small interfering RNA (siRNA) targeting human Nrf2 (5'-GAGUACAGUGUCUUAUA-3') and a non-sense control siRNA (5'-UUCUCCGAACGUGUCACGUTT-3') were purchased from Shanghai GenePharma Co., Ltd. BEL-7402/ADM cells were seeded at  $1.5 \times 10^5$  cells/well into 6-well plates. The following day, cells were transfected with 5nM of Nrf2 siRNA using HiPerFect Transfection reagent according to the manufacturer's instructions.

#### Real-time quantitative PCR

Total cellular RNA was extracted using the TRIzol reagent according to the manufacturer's protocol. qPCR was performed using SLAN real-time PCR detection system with the following cycles: 95°C for 1 min; 95°C for 15 s, 58°C for 20 s and 72°C for 20 s (40 cycles); and 72°C for 5 min. Primer sequences were Nrf2: 5'-TGA GGT TTC TTC GGC TAC GTT-3' (forward) and 5'-CTT CTG TCA GTT TGG CTT CTG G-3' (reverse); HO-1: 5'-CTG GAG GAG ATT GAG CG-3' (forward) and 5'-ATG GCT GGT GTG TAG GGG AT-3' (reverse); MRP5: 5'-ACT CGA CCG TTG GAA TGC C-3' (forward) and 5'-GGG TGC TGG TGT TTG GAA GT-3' (reverse);

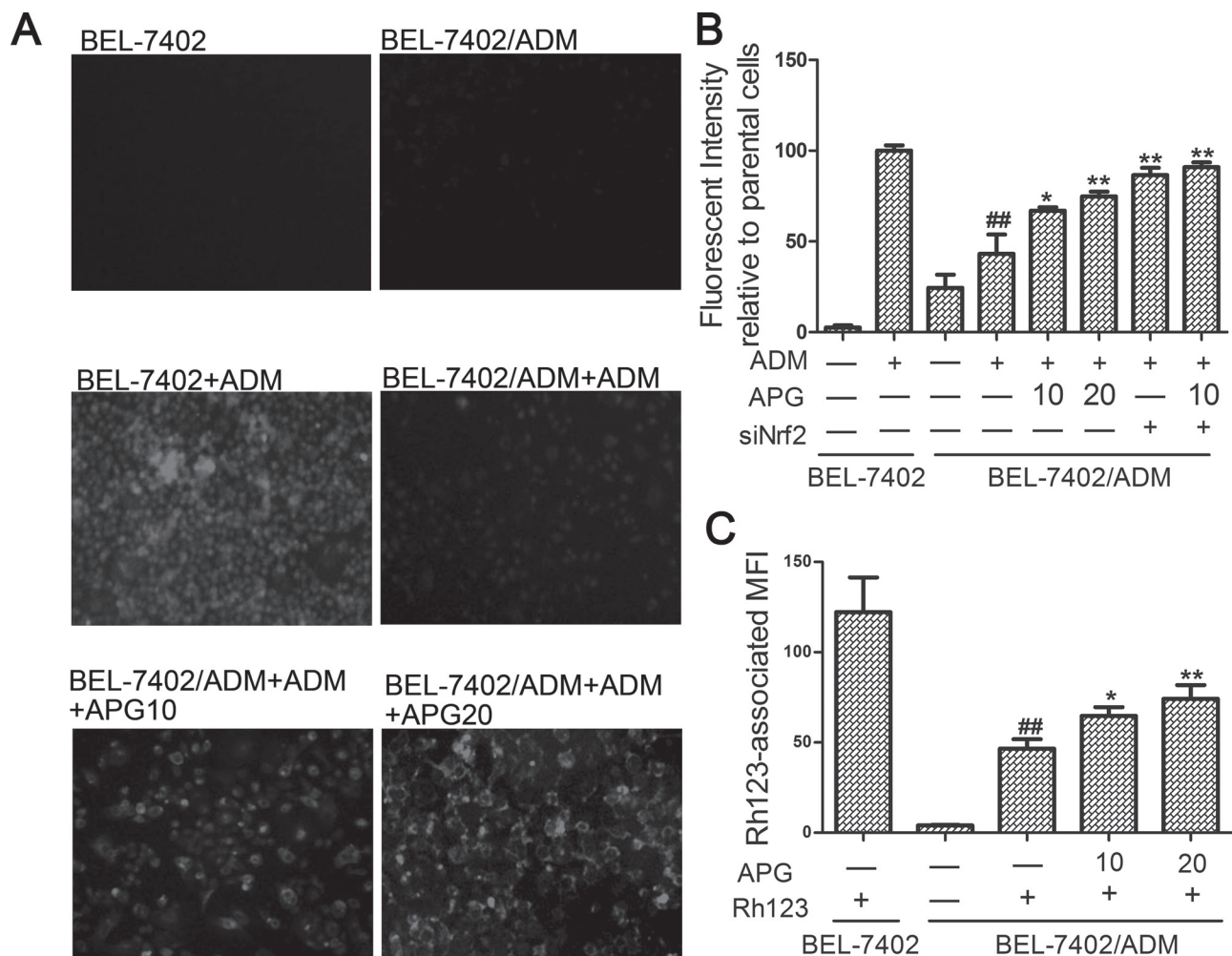


**Fig. 2.** APG increased intracellular accumulation of ADM in BEL-7402/ADM cells. (A) BEL-7402/ADM cells were treated with ADM (8  $\mu\text{M}$ ) for 3h following 24h of exposure to APG (10 and 20  $\mu\text{M}$ ). The fluorescence intensity of intracellular ADM was directly observed by fluorescence microscopy. All images are shown at  $\times 200$ . (B) Intracellular accumulation of ADM analyzed by FCM. Results are presented as fold change in fluorescence intensity relative to control BEL-7402 cells.  $##P < 0.01$  versus parental + ADM;  $*P < 0.05$ ,  $**P < 0.01$  versus resistance + ADM. (C) Effect of APG on the accumulation of Rh123 in BEL-7402/ADM cells. Cells were incubated with 5  $\mu\text{g/ml}$  of Rh123 for 1h following 24h of exposure to APG (10 and 20  $\mu\text{M}$ ). Data are expressed as mean  $\pm$  SD ( $n = 3$ ).  $##P < 0.01$  versus parental + Rh123;  $*P < 0.05$ ,  $**P < 0.01$  versus resistance + Rh123.

AKR1B10: 5'-AGC AGG ACG TGA GAC TTC TAC CTG C-3' (forward) and 5'-TCC ACC GAT GGC ATT ACC TTT A-3' (reverse); Keap1: 5'-CCT TCA GCT ACA CCC TGG AG-3' (forward) and 5'-AAC ATG GCC TTG AAG ACA GG-3' (reverse); and  $\beta$ -actin: 5'-GTC CAC CGC AAA TGC TTC T A-3' (forward) and 5'-TGC TGT CAC CTT CAC CGT TC-3' (reverse). The data were collected and calculated using the comparative Ct method and normalized to  $\beta$ -actin.

**Immunofluorescence assay**

Cells were fixed using 4% paraformaldehyde for 20 min, permeabilized with 0.3% Triton X-100 for 20 min, blocked in PBS with 30% fetal bovine serum for 30 min followed by incubation with Nrf2 antibody (1:50) at 4°C for 24h, washed with PBS and labeled with a fluorescein isothiocyanate-conjugated anti-rabbit immunoglobulin G antibody (1:100) at room temperature for 1h. Nuclei were counterstained with DAPI (1  $\mu$ g/ml) for 5 min. Cells were examined under a fluorescence microscope.

**Western blot analysis**

Whole-cell extracts and nuclear extracts were prepared. Protein samples were resolved in 12% sodium dodecyl sulfate-polyacrylamide gels and transferred onto polyvinylidene difluoride membranes. After successful transfer of proteins, the membranes were blocked with 5% skim milk at room temperature for 2h. Primary antibody incubation was carried out at 4°C overnight followed by incubation with secondary antibody conjugated to horseradish peroxidase for

1.5h. Bands were visualized with an enhanced chemiluminescence detection kit following the manufacturer's instructions.

**In vivo xenograft studies**

Male BALB/c nude mice (20  $\pm$  5 g, 5 weeks old) were purchased from Beijing HFK Bioscience Co. Ltd. All animal procedures were approved by the animal ethics committee of Hubei University of Medicine. Mice were injected with BEL-7402 (200  $\mu$ l,  $1 \times 10^7$  cells) in the subdermal space on the right flanks. Once tumors grew to the desired size, mice were randomly assigned into four groups and treated intraperitoneally with vehicle, ADM (3 mg/kg), APG (50 mg/kg) or in combination every 3 days for a total of seven times. Tumor volume was measured semiweekly and calculated using the formula  $(a \times a \times b)/2$  ( $a$ , the smallest diameter;  $b$ , the largest diameter). Upon termination, tumors were harvested, and proteins were extracted for western blot. Formalin-fixed, paraffin-embedded tumor tissue sections were used for Ki-67 and terminal deoxynucleotidyl transferase-mediated dUTP nick end labeling analysis.

**Statistical analysis**

Experiments were performed in triplicate and data were expressed as mean  $\pm$  SD. Statistical significance was determined by Student's  $t$ -test or one-way analysis of variance.  $P < 0.05$  was considered statistically significant.

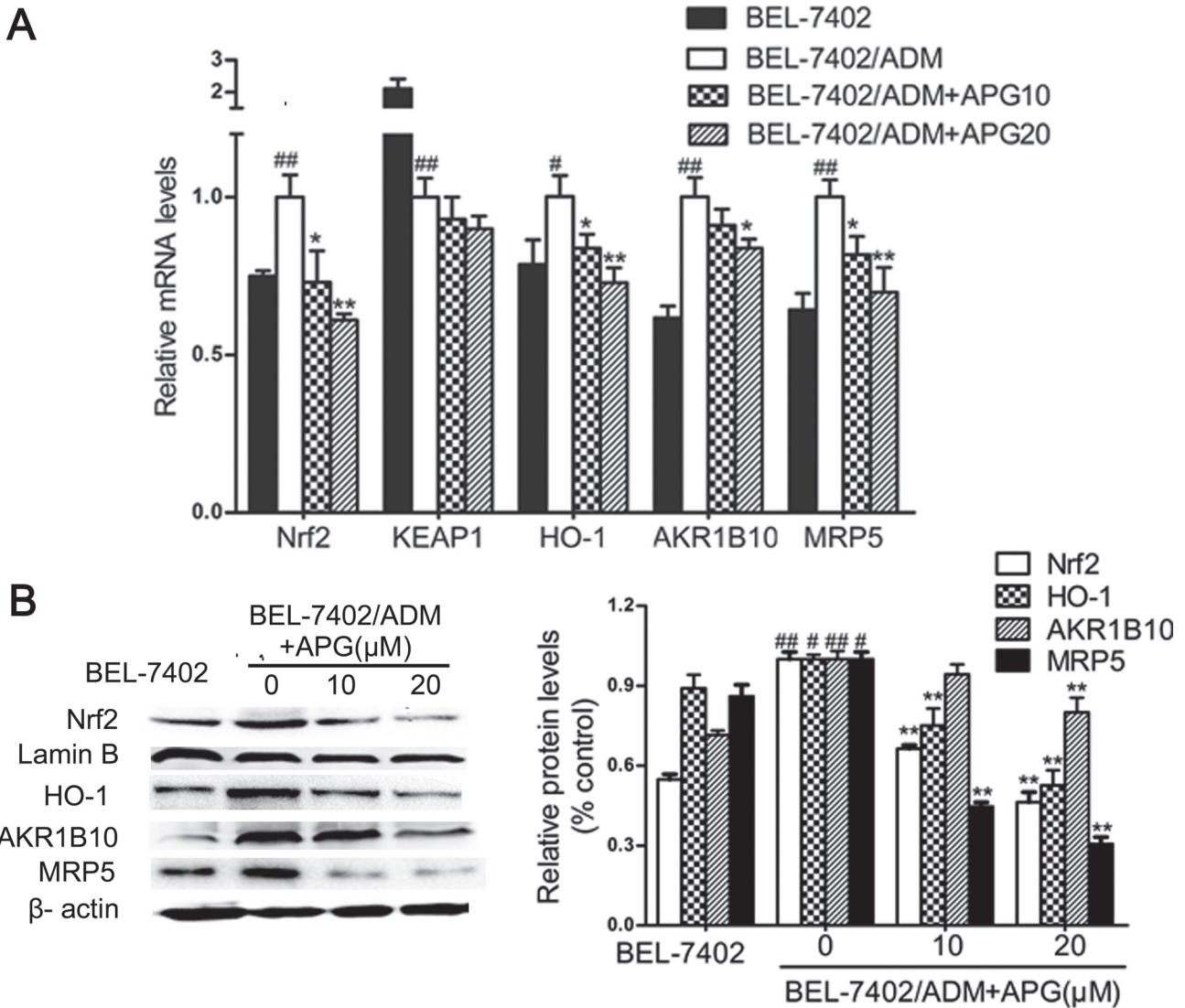


**Fig. 3.** Dose-dependent effect of APG on mRNA and nuclear protein expression of Nrf2, HO-1, AKR1B10 and MRP5 in BEL-7402/ADM cells. (A) Cells were treated with APG (10 and 20  $\mu$ M) for 24h and subjected to real-time quantitative PCR. (B) BEL-7402/ADM cells were treated with APG (10 and 20  $\mu$ M) for 24h prior to western blot. Data are expressed as mean  $\pm$  SD ( $n = 3$ ). # $P < 0.05$ , ## $P < 0.01$  versus parental, \* $P < 0.05$ , \*\* $P < 0.01$  versus resistance.

## Results

### APG enhances sensitivity of BEL-7402/ADM cells to ADM

Cells were exposed to ADM in the presence of 10  $\mu\text{M}$  APG, as low cytotoxicity occurred at this concentration (Figure 1A). APG markedly enhanced the cytotoxicity of ADM to BEL-7402/ADM cells (Figure 1C). Results from the experiment showed that the  $\text{IC}_{50}$  value of ADM for BEL-7402/ADM cells was 3.41 times that for BEL-7402 cells (Figure 1B). The reversal index was 3.04-fold by APG at the concentration of 10  $\mu\text{M}$  for ADM (Figure 1C). Additionally, the effect of APG on cell growth and apoptosis was also investigated. APG caused a significant accumulation of BEL-7402/ADM cells in the S-phase of the cell cycle (Figure 1D). DAPI assay showed that all treated cells have chromosomal condensation and formation of apoptotic bodies and the most obvious phenomenon is observed in cotreated group (Figure 1E).

### APG increases intracellular accumulation of ADM

To confirm the chemosensitivity was eventually due to increased intracellular drug concentration, fluorometric and FCM analyses were performed to measure intracellular ADM concentration. As shown in Figure 2A, BEL-7402/ADM cells incubated with APG emitted higher fluorescence intensity compared with free APG. In agreement with the observations in fluorometric analysis, FCM analysis also showed that APG can enhance intracellular ADM accumulation, and the effect augmented with the concentration of APG. The fluorescence intensity of ADM in 20  $\mu\text{M}$  APG-treated BEL-7402/ADM cells increased 30% compared with the untreated cells (Figure 2B). We also conducted transport assay to analyze the effects of APG on the accumulation of Rh123 (a fluorescent

P-gp substrate). As shown in Figure 2C, the fluorescence intensity of Rh123 in BEL-7402 and BEL-7402/ADM cells was 122.17 and 46.6 U, respectively ( $P < 0.01$ ). APG could significantly increase the intracellular Rh123 accumulation in BEL-7402/ADM cells ( $P < 0.05$ ,  $P < 0.01$ ). The fluorescence intensity of Rh123 in 20  $\mu\text{M}$  APG-treated cells was 74.13 U, which was 59% higher than that of untreated cells. Taken together, these data indicate that APG elevates the cytotoxicity of ADM toward BEL-7402/ADM cells through increasing intracellular accumulation of ADM.

### APG inhibits the Nrf2 signaling pathway

Real-time quantitative PCR analysis revealed that APG suppressed the messenger RNA (mRNA) expression of HO-1, AKR1B10 and MRP5 in a dose-dependent manner. Twenty micromolar of APG reduced the mRNA levels of these genes by 27, 16 and 30%, respectively. Interestingly, Nrf2 mRNA was downregulated even more than its target genes. In BEL-7402/ADM cells, Nrf2 mRNA level dropped more than 39% in the presence of 20  $\mu\text{M}$  APG (Figure 3A). In contrast, Keap1 mRNA level was not affected, suggesting that APG-mediated inhibition is independent of Keap1. In addition, APG reduced protein levels of nuclear Nrf2 as well as Nrf2-target genes, including HO-1, AKR1B10 and MRP5 in a dose-dependent manner, consistent with their mRNA expressions (Figure 3B). Taken together, these results suggest that APG inhibits transcription of the ARE-driven genes in BEL-7402/ADM cells.

### APG increases the sensitivity of BEL-7402/ADM cells to ADM by inhibition of Nrf2

To determine if Nrf2 signaling pathway is involved in APG-increased sensitivity of BEL-7402/ADM cells to ADM, BEL-7402/ADM cells were transfected with Nrf2 siRNA to knockdown Nrf2

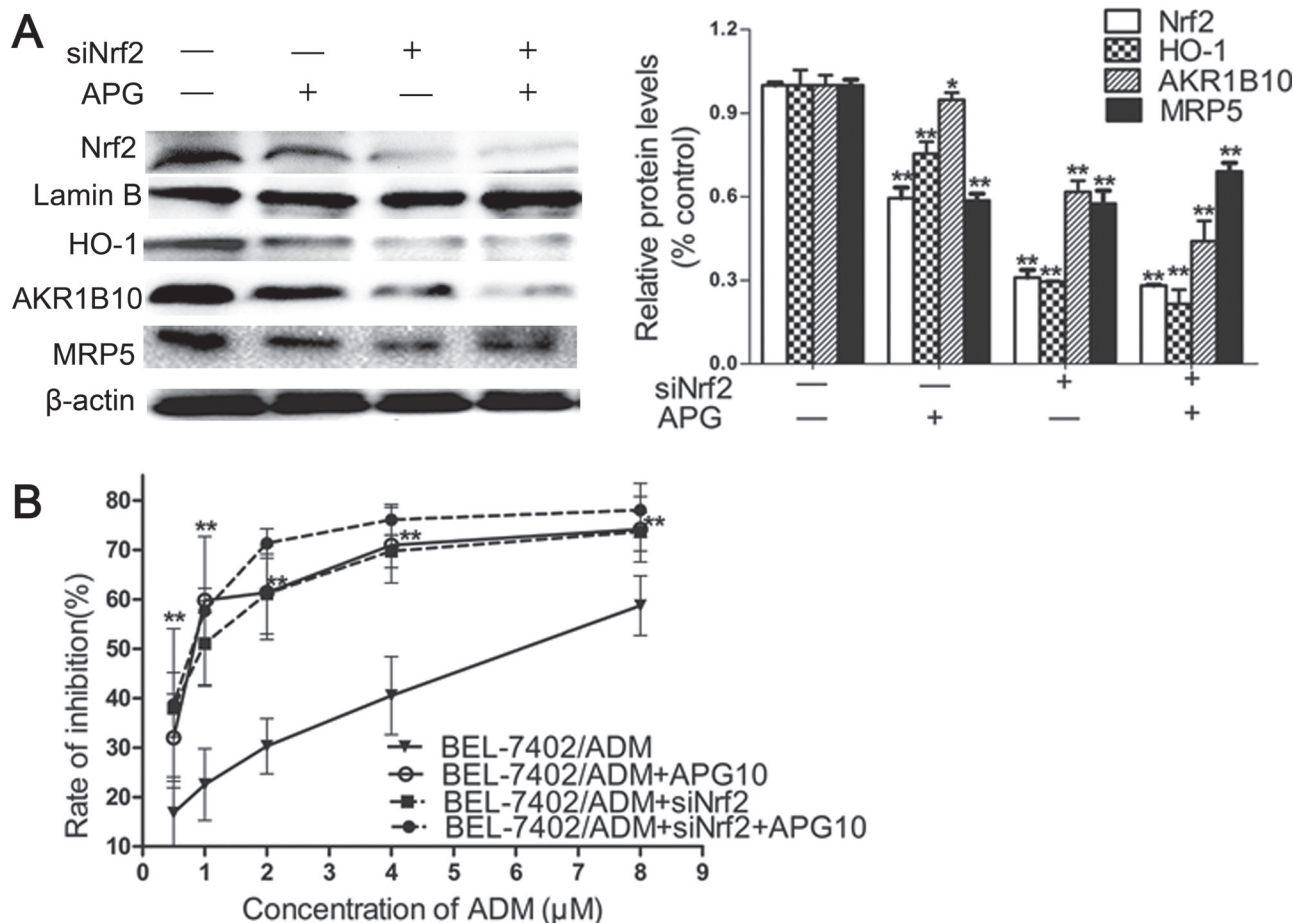


**Fig. 4.** APG increased the sensitivity of BEL-7402/ADM cells to ADM by inhibition of Nrf2. (A) Effect of Nrf2 knockdown on drug-resistant gene protein expression. \* $P < 0.05$ , \*\* $P < 0.01$  versus resistance. (B) Effect of Nrf2 knockdown on the sensitivity to ADM. Cells were pretreated with 10  $\mu\text{M}$  of APG for 24 h prior to 48 h exposure to ADM (0.5–8  $\mu\text{M}$ ). Cell viability was monitored by MTT assay. Data are expressed as mean  $\pm$  SD ( $n = 3$ ).

expression. Western blot confirmed the successful knockdown of Nrf2 in BEL-7402/ADM cells. The expression of Nrf2-target genes HO-1, AKR1B10 and MRP5 was also reduced significantly in these cells. Moreover, APG did not significantly change levels of nuclear Nrf2 protein and its downstream genes in BEL-7402/ADM cells transfected with Nrf2 siRNA (Figure 4A). As shown in Figure 2B, intracellular accumulation of ADM increased 43% after transfection

with Nrf2 siRNA compared with the untreated cells, but accumulation of ADM was nearly identical in the presence or absence of APG in BEL-7402/ADM cells with Nrf2 knockdown. These data suggest that inhibiting Nrf2 contributes to increasing accumulation of ADM in BEL-7402/ADM cells by APG.

To confirm if the sensitization by APG was Nrf2 dependent, we tested the sensitivity of BEL-7402/ADM cells to ADM with

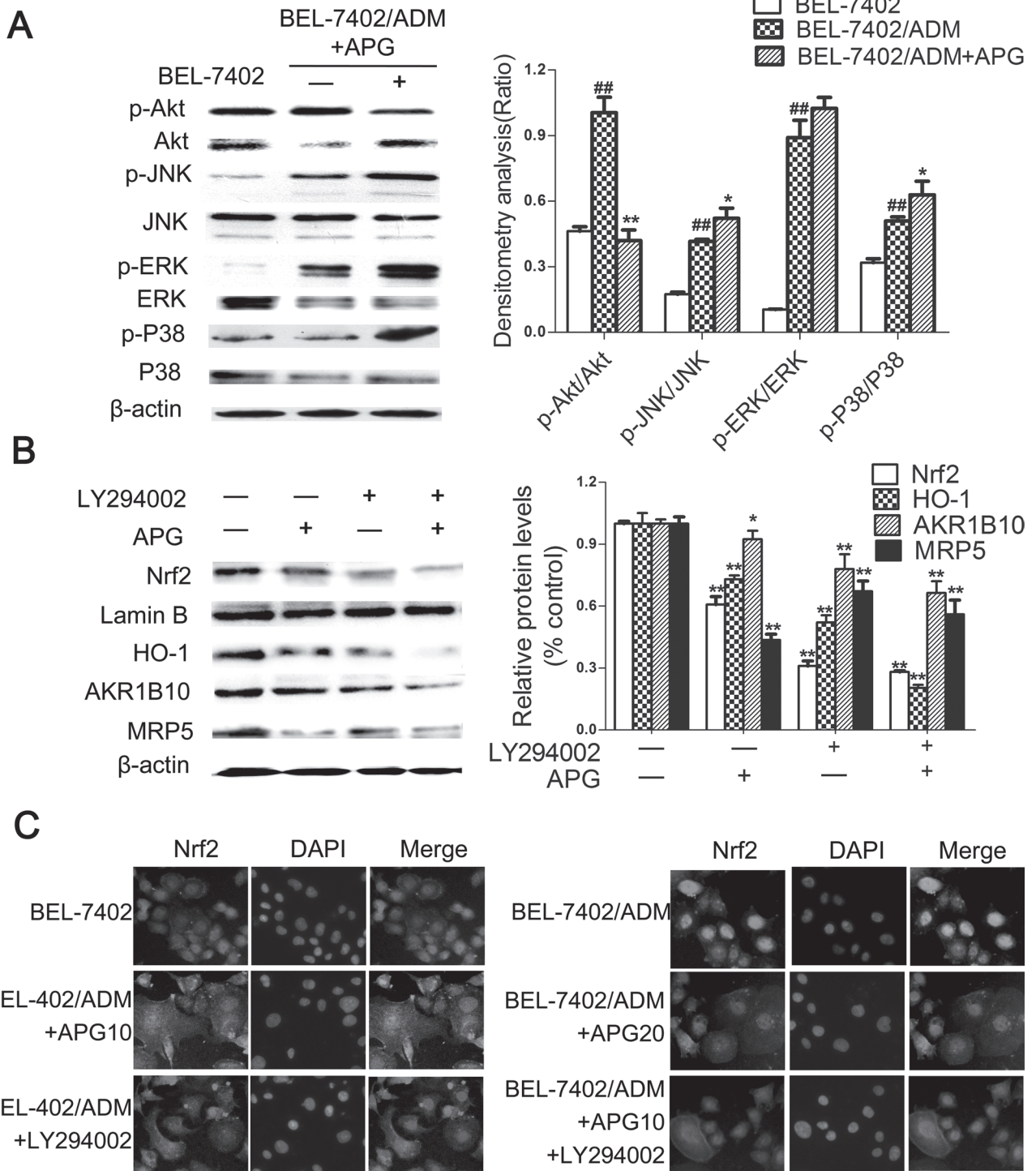


**Fig. 5.** Inhibition of PI3K reduced Nrf2-mediated response in BEL-7402/ADM cells. (A) APG suppressed p-Akt in BEL-7402/ADM cells. Reduced expression of p-Akt and increased expression of p-P38, p-JNK and p-ERK1/2 were observed after exposure to APG (20 μM) for 24h. ##*P* < 0.01 versus parental; \**P* < 0.05, \*\**P* < 0.01 versus resistance. (B) LY294002 (50 μM) reduced the protein levels of nuclear Nrf2 and Nrf2-target genes including HO-1, AKR1B10 and MRP5. \**P* < 0.05, \*\**P* < 0.01 versus resistance. (C) BEL-7402/ADM cells were pretreated with LY294002 (50 μM) or/and APG for 24h prior to fluorescence microscopy. All images are shown at ×200.

Nrf2 knockdown. In agreement with the results in Figure 2B, Nrf2 siRNA-transfected BEL-7402/ADM cells were much more sensitive to ADM than BEL-7402/ADM cells. However, the effect of APG was diminished in Nrf2 siRNA-transfected BEL-7402/ADM cells (Figure 4B). These data further demonstrate that APG increases the sensitivity of BEL-7402/ADM cells to ADM by inhibition of Nrf2.

#### APG downregulates Nrf2 pathway through inhibiting PI3K/Akt pathway

Mitogen-activated protein kinases and PI3K/Akt signaling pathways have been found to be involved in chemoresistance. To determine the mechanism of APG in sensitizing BEL-7402/ADM cells, the effects of APG on the mitogen-activated protein kinase and Akt pathways were studied. As shown in Figure 5, APG attenuated expression of p-Akt and increased p-P38, p-JNK and p-ERK1/2 levels. Importantly, inhibition of PI3K signaling by PI3K inhibitor LY294002 reduced the protein levels of nuclear Nrf2 and Nrf2-target genes including HO-1, AKR1B10 and MRP5. Interestingly, APG did not significantly change LY294002-reduced Nrf2 expression (Figure 5B). Furthermore, LY294002 inhibited Nrf2 translocation into the nucleus. It appeared that APG was unable to remove LY294002-mediated inhibition (Figure 5C). Collectively, these data suggest that APG inhibits Nrf2 expression through PI3K/Akt signaling pathways.

#### APG sensitizes BEL-7402 cell xenografts to ADM treatment

To elucidate whether APG and ADM can act synergistically *in vivo*, we transplanted BEL-7402 cells into mice bearing subcutaneous tumors. As shown in Figure 6, APG or ADM alone inhibited tumor weight by 40 or 55% on day 40. However, combination of ADM and APG reduced the tumor size by 64%. In the molecular level, APG alone or combined treatment significantly inhibited Nrf2 expression in the tumor tissues (Figure 6C). Although ADM treatment inhibited cell proliferation slightly, there was a significant decrease in cell proliferation when cells were cotreated with both ADM and APG. Furthermore, APG alone induced slight apoptosis, whereas the combined treatment significantly induced a large number of apoptotic cells (Supplementary Figure S2, available at *Carcinogenesis* Online). Our findings strongly support that combination of ADM and APG can significantly suppress HCC growth by reducing cell proliferation and inducing apoptosis *in vivo*.

#### Discussion

Drug resistance during chemotherapy is the major obstacle to the successful treatment of many cancers. Nrf2 has been proposed as a novel therapeutic target to overcome chemoresistance. In the present study, overexpression of Nrf2 and its downstream genes AKR1B10 and MRP5 was detected in human HCC tissues compared with those in the matched adjacent non-neoplastic liver tissues (Supplementary Figure S1, available at *Carcinogenesis* Online). The positive

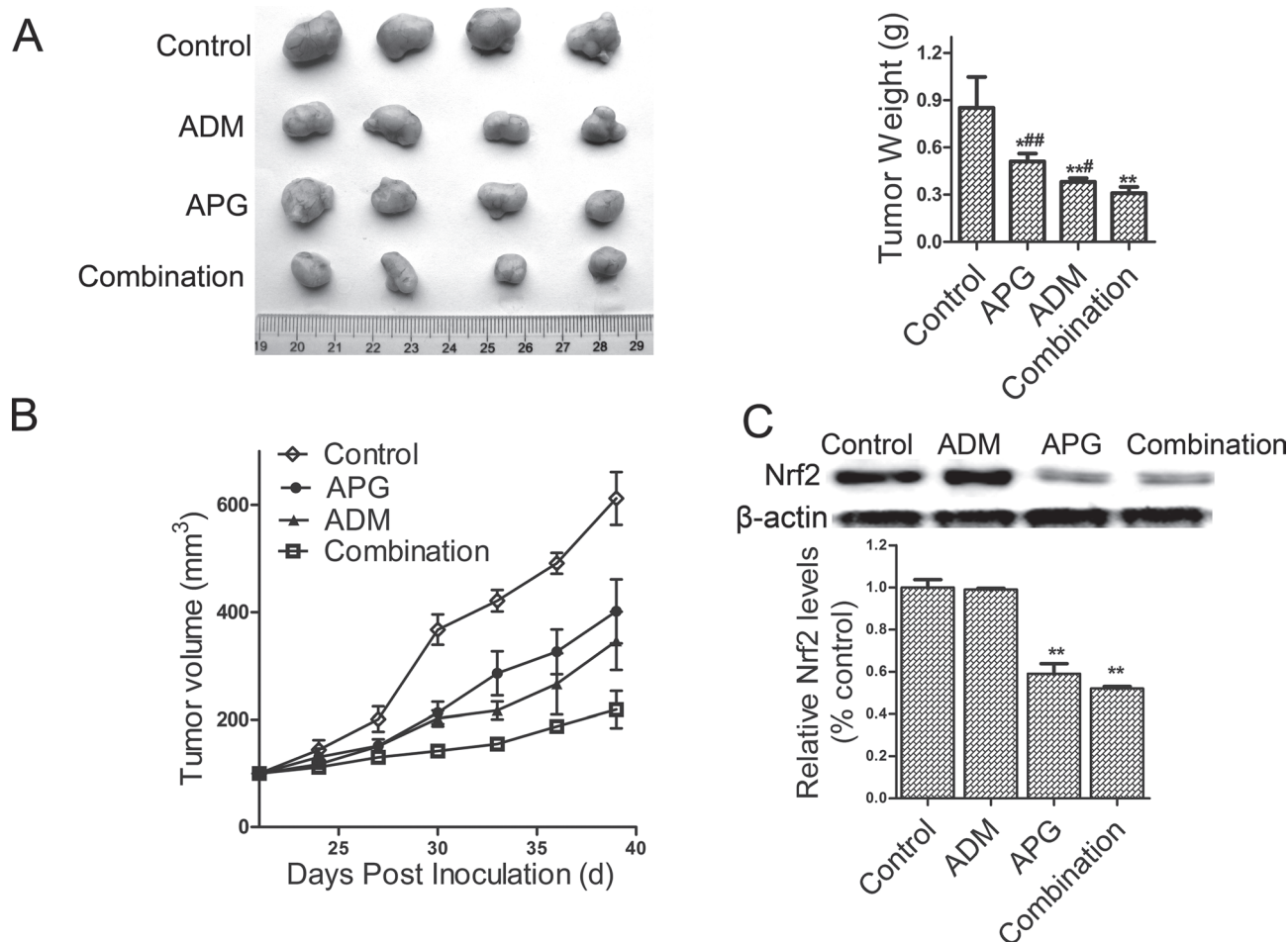


**Fig. 6.** APG sensitized BEL-7402 xenografts to ADM treatment. (A) Combined treatment with APG and ADM significantly reduced tumor weight. When tumor size reached 100 mm<sup>3</sup>, mice (eight per group) were treated with vehicle, ADM (3 mg/kg), APG (50 mg/kg) or both APG and ADM through intraperitoneally every 3 days for a total of seven times. Tumors were excised and weighed at the end of the experiment (40 days). (B) Combined treatment with APG and ADM significantly inhibited tumor growth. Tumor sizes were measured semiweekly. (C) APG reduced Nrf2 expression in xenografts *in vivo*. \**P* < 0.05, \*\**P* < 0.01 versus vehicle control; #*P* < 0.05, ##*P* < 0.01 vs combination.

correlation between Nrf2 and AKR1B10/MRP5 protein levels was also shown in these tissues (Supplementary Table S1, available at *Carcinogenesis* Online). Furthermore, remarkable higher levels of Nrf2 and its target proteins were detected in BEL-7402/ADM cells as compared with BEL-7402 cells (Figure 3). On the other hand, intracellular Nrf2 protein and its downstream gene expression were significantly decreased, and ADM resistance was partially reversed by Nrf2 siRNA in BEL-7402/ADM cells (Figure 4). Our findings suggest an important role of Nrf2 in chemoresistance of human HCC, and the induction of target proteins by Nrf2 activation might be involved in the process. Therefore, identification of potent small-molecule inhibitors of Nrf2 is urgently needed.

Previously, we identified several small-molecule inhibitors of Nrf2. Luteolin was a potent small-molecule inhibitor of Nrf2, which acts as effectively as Nrf2 siRNA in downregulating cytoprotective enzymes, depleting glutathione and sensitizing non-small cell lung cancer cells to anticancer drugs (19). Brusatol acted as a unique inhibitor of the Nrf2 pathway that sensitizes a broad spectrum of cancer cells and A549 xenografts to cisplatin and other chemotherapeutic drugs (20). Epigallocatechin 3-gallate was found to suppress Nrf2 activity and reduce HO-1 expression in A549 cells, although the concentrations of epigallocatechin 3-gallate required for its inhibitory effect were high (>200  $\mu$ M) (18).

In this study, we discovered a potent small-molecule inhibitor of Nrf2, APG. Similar to luteolin, brusatol and epigallocatechin 3-gallate, APG is a natural compound with anticancer potential. APG enhanced the cytotoxicity of anticancer drugs and increased intracellular concentration of ADM in chemoresistant cancer cells that overexpress Nrf2. No obvious toxicity was observed at the doses that were sufficient to sensitize cancer cells to chemotherapeutic treatments. APG-mediated sensitization to ADM relies on its ability to suppress Nrf2 pathway through reducing nuclear Nrf2 protein level as well as xenobiotic metabolizing and antioxidant enzymes (HO-1, AKR1B10 and MRP5) in BEL-7402/ADM cells (Figure 3). Although Keap1 suppressed Nrf2 expression, APG did not alter Keap1 mRNA expression while inhibiting Nrf2 expression (Figure 3A), suggesting that APG may inhibit Nrf2 expression through a different mechanism. Indeed, we found that APG inhibited Nrf2 expression through PI3/Akt signaling pathway. In addition, APG and ADM cotreatment inhibited tumor growth, reduced cell proliferation and induced apoptosis more substantially when compared with ADM treatment alone in BEL-7402 xenografts. These findings suggest that APG could be a useful tool for dissecting the Nrf2/ARE pathway and indicate the potential of this flavonoid for further therapeutic development.

Interestingly, Huang *et al.* (23) demonstrated that in rat primary hepatocytes, APG is shown to have opposite effect, activating Nrf2 nuclear translocation, nuclear Nrf2-ARE binding activity and ARE-dependent luciferase activity. Thus, the actions of APG on the Nrf2/ARE pathway appear to have multiple mechanisms and are cell-type specific. The differential actions of APG on the Nrf2/ARE signalling pathway could be aspects of its chemopreventive and chemotherapeutic potential.

Recent studies have reported that the Nrf2 pathway is also tightly regulated by other signaling pathways. Nrf2 activity is antagonized by a variety of transcription factors such as activating transcription factor 3, estrogen receptor  $\alpha$  and peroxisome proliferator-activated receptor (24). Therefore, it is possible to downregulate Nrf2 pathway by treating cancer cells with agents that activate activating transcription factor 3, estrogen receptor  $\alpha$  or peroxisome proliferator-activated receptor  $\gamma$ . Whether these transcription factors are implicated in the modulation of Nrf2 pathway by APG remains to be investigated.

Our study also addresses another important issue. Many studies have suggested that the beneficial effects of chemopreventive drugs on suppression of carcinogenesis are mediated through activation of Nrf2. However, a recent genetic analysis of human tumors has indicated that Nrf2 may conversely promote oncogenesis and cause chemoresistance. It is therefore controversial whether the activation, or alternatively the inhibition, of Nrf2 is a useful strategy for the prevention or treatment of cancer. We would suggest that both sides

of the argument over this apparent paradox have merit, but the answer may depend on the context (25).

In conclusion, the present study demonstrates that BEL-7402/ADM cells acquiring resistance to chemotherapeutic agents due to Nrf2 overexpression become susceptible by the drug treatment combined with APG. APG downregulates HO-1, AKR1B10 and MRP5 by suppressing PI3K/AKT/Nrf2 pathway, thus, reverses the drug-resistant phenotype. Further studies in human clinical trials are necessary in order to exploit this flavonoid as a possible natural agent for the prevention and treatment of cancer.

### Supplementary material

Supplementary Figures S1 and S2 and Table S1 can be found at <http://carcin.oxfordjournals.org/>

### Funding

National Natural Science Foundation of China (30973586).

### Acknowledgement

We thank Professor X.B.Wang (Laboratory of Chinese Herbal Pharmacology, Hubei University of Medicine) for the generous gift of BEL-7402/ADM and BEL-7402 cells and critically reading this manuscript.

*Conflict of Interest Statement:* None declared.

### References

- Yang, J.D. *et al.* (2010) Hepatocellular carcinoma: a global view. *Nat. Rev. Gastroenterol. Hepatol.*, **7**, 448–458.
- Kensler, T.W. *et al.* (2007) Cell survival responses to environmental stresses via the Keap1–Nrf2–ARE pathway. *Annu. Rev. Pharmacol. Toxicol.*, **47**, 89–116.
- Shen, K. *et al.* (2012) Inhibition of IGF-IR increases chemosensitivity in human colorectal cancer cells through MRP-2 promoter suppression. *J. Cell. Biochem.*, **113**, 2086–2097.
- Itoh, K. *et al.* (2010) Discovery of the negative regulator of Nrf2, Keap1: a historical overview. *Antioxid. Redox Signal.*, **13**, 1665–1678.
- Al-Mulla, F. *et al.* (2012) A new model for raf kinase inhibitory protein induced chemotherapeutic resistance. *PLoS One*, **7**, e29532.
- Wang, X.J. *et al.* (2008) Nrf2 enhances resistance of cancer cells to chemotherapeutic drugs, the dark side of Nrf2. *Carcinogenesis*, **29**, 1235–1243.
- Zhang, P. *et al.* (2010) Loss of Kelch-like ECH-associated protein 1 function in prostate cancer cells causes chemoresistance and radioresistance and promotes tumor growth. *Mol. Cancer Ther.*, **9**, 336–346.
- Homma, S. *et al.* (2009) Nrf2 enhances cell proliferation and resistance to anticancer drugs in human lung cancer. *Clin. Cancer Res.*, **15**, 3423–3432.
- Cho, J.M. *et al.* (2008) Role of the Nrf2-antioxidant system in cytotoxicity mediated by anticancer cisplatin: implication to cancer cell resistance. *Cancer Lett.*, **260**, 96–108.
- Hong, Y.B. *et al.* (2010) Nuclear factor (erythroid-derived 2)-like 2 regulates drug resistance in pancreatic cancer cells. *Pancreas*, **39**, 463–472.
- Fukumoto, S. *et al.* (2007) Overexpression of the aldo-keto reductase family protein AKR1B10 is highly correlated with smokers' non small cell lung carcinomas. *Int. J. Gynecol. Cancer*, **17**, 1300–1306.
- Heringlake, S. *et al.* (2010) Identification and expression analysis of the aldo-keto reductase 1B10 gene in primary malignant liver tumours. *J. Hepatol.*, **52**, 220–227.
- Nishinaka, T. *et al.* (2011) Regulation of aldo-keto reductase AKR1B10 gene expression: involvement of transcription factor Nrf2. *Chem. Biol. Interact.*, **191**, 185–191.
- Liu, Z. *et al.* (2012) Epidermal growth factor induces tumour marker AKR1B10 expression through activator protein-1 signalling in hepatocellular carcinoma cells. *Biochem. J.*, **442**, 273–282.
- Bacolod, M.D. *et al.* (2008) The gene expression profiles of medulloblastoma cell lines resistant to preactivated cyclophosphamide. *Curr. Cancer Drug Targets*, **8**, 172–179.
- Matsunaga, T. *et al.* (2011) Involvement of the aldo-keto reductase, AKR1B10, in mitomycin-c resistance through reactive oxygen species-dependent mechanisms. *Anticancer Drugs*, **22**, 402–408.

17. Nambaru, P.K. *et al.* (2011) Drug efflux transporter multidrug resistance-associated protein 5 affects sensitivity of pancreatic cancer cell lines to the nucleoside anticancer drug 5-fluorouracil. *Drug Metab. Dispos.*, **39**, 132–139.
18. Kweon, M.H. *et al.* (2006) Constitutive overexpression of Nrf2-dependent heme oxygenase-1 in A549 cells contributes to resistance to apoptosis induced by epigallocatechin 3-gallate. *J. Biol. Chem.*, **281**, 33761–33772.
19. Tang, X. *et al.* (2011) Luteolin inhibits Nrf2 leading to negative regulation of the Nrf2/ARE pathway and sensitization of human lung carcinoma A549 cells to therapeutic drugs. *Free Radic. Biol. Med.*, **50**, 1599–1609.
20. Ren, D. *et al.* (2011) Brusatol enhances the efficacy of chemotherapy by inhibiting the Nrf2-mediated defense mechanism. *Proc. Natl Acad. Sci. USA*, **108**, 1433–1438.
21. Seo, Y.J. *et al.* (2011) Apoptotic effects of genistein, biochanin-A and apigenin on LNCaP and PC-3 cells by p21 through transcriptional inhibition of polo-like kinase-1. *J. Korean Med. Sci.*, **26**, 1489–1494.
22. Wang, X.B. *et al.* (2010) Inhibition of tetramethylpyrazine on P-gp, MRP2, MRP3 and MRP5 in multidrug resistant human hepatocellular carcinoma cells. *Oncol. Rep.*, **23**, 211–215.
23. Huang, C.S. *et al.* (2013) Protection by chrysin, apigenin, and luteolin against oxidative stress is mediated by the Nrf2-dependent up-regulation of heme oxygenase 1 and glutamate cysteine ligase in rat primary hepatocytes. *Arch. Toxicol.*, **87**, 167–178.
24. Hayes, J.D. *et al.* (2009) NRF2 and KEAP1 mutations: permanent activation of an adaptive response in cancer. *Trends Biochem. Sci.*, **34**, 176–188.
25. Sporn, M.B. *et al.* (2012) NRF2 and cancer: the good, the bad and the importance of context. *Nat. Rev. Cancer*, **12**, 564–571.

Received October 29, 2012; revised March 5, 2013; accepted March 29, 2013